Journal of Power Sources 269 (2014) 812–817

Contents lists available at ScienceDirect

Journal of Power Sources

journal homepage: www.elsevier.com/locate/jpowsour

Impregnated $Nd_2NiO_{4+\delta}$- scandia stabilized zirconia composite cathode for intermediate-temperature solid oxide fuel cells

Ting Chen [a], Yucun Zhou [a], Chun Yuan [a], Minquan Liu [a], Xie Meng [a], Zhongliang Zhan [a, b], Changrong Xia [a, b], Shaorong Wang [a, b, *]

[a] CAS Key Laboratory of Materials for Energy Conversion, Shanghai Institute of Ceramics, Chinese Academy of Sciences (SICCAS), 1295 Dingxi Road, Shanghai 200050, PR China
[b] Department of Material Science and Engineering, University of Science and Technology of China, 96 Jinzhai Road, Hefei, Anhui 230026, PR China

HIGHLIGHTS

- Novel $Nd_2NiO_{4+\delta}$-SSZ composite cathode is prepared.
- Impregnated $Nd_2NiO_{4+\delta}$ cathode shows a low ASR of 0.04 Ω cm^2 at 800 °C.
- Maximum power density of 1.26 W cm^{-2} is obtained at 800 °C for IT-SOFCs.

ARTICLE INFO

Article history:
Received 24 June 2014
Received in revised form
10 July 2014
Accepted 11 July 2014
Available online 19 July 2014

Keywords:
Solid oxide fuel cell
Cathode
Nickelate oxide
Impregnation

ABSTRACT

Here we developed a novel $Nd_2NiO_{4+\delta}$ (NNO) impregnated SSZ composite cathode for intermediate temperature solid oxide fuel cells (IT-SOFCs). The area specific polarization resistance of the composite cathode for oxygen reduction can be as low as 0.04 Ω cm^2 at 800 °C. The anode supported SOFC with the structure of Ni-YSZ anode, SSZ electrolyte and impregnated NNO-SSZ composite cathode was prepared by the tape casting, co-firing and impregnation method. The resulting fuel cell exhibits maximum power densities of 1.26 and 0.73 W cm^{-2} at 800 and 700 °C, respectively when operated in hydrogen and air. Additionally, the electrical conductivity of the NNO cathode and the chemical compatibility with the electrolyte material were also studied.

1. Introduction

Solid oxide fuel cells (SOFCs) have been attracting much attention in recent decades for the advantages like high efficiency, low pollution, fuel flexibility and all-solid-state structure [1–3]. However, the commercialization of SOFC technology is hindered by the high manufacturing cost, insufficient long-term operation stability and system reliability [4,5]. Lowering the operating temperature of SOFCs from the traditional 900–1000 °C to 600–800 °C can reduce the system cost and increase the performance durability [6]. Nevertheless, the overall electrochemical performance of the SOFCs becomes poor at a lower operating temperature due to the increased ohmic resistance mainly from the electrolyte and the polarization resistances from the electrodes. Applying the nano-scale thin electrolyte film prepared by pulsed laser deposition (PLD) or other deposition techniques can greatly reduce the ohmic resistance [7,8], while such techniques are not appropriate to be used for mass production due to their high equipment cost and low deposition efficiency. Meanwhile, the ultrathin electrolyte film with low mechanic reliability has the risk of cracking in practical application. By using highly conductive electrolytes, such as doped ceria and strontium- and magnesium-doped lanthanum gallate (LSGM), we can also reduce the ohmic resistance [9,10], but doped ceria has electronic conductivity in reducing atmosphere and LSGM has the drawbacks like poor stability, high material cost and fairly reactivity with the Ni-based anode [11]. On the other hand, in order to solve the problem of increased polarization resistances at a lower operating temperature, both the electrode materials and the electrode structure should be taken into account, especially for the cathode. Novel cathode materials with high performance have been developed to decrease the polarization resistance at low operating

* Corresponding author. CAS Key Laboratory of Materials for Energy Conversion, Shanghai Institute of Ceramics, Chinese Academy of Sciences (SICCAS), 1295 Dingxi Road, Shanghai 200050, PR China. Tel.: +86 21 5241 1520; fax: +86 21 5241 3903.
E-mail address: srwang@mail.sic.ac.cn (S. Wang).

http://dx.doi.org/10.1016/j.jpowsour.2014.07.073
0378-7753/

temperatures [12,13] and the impregnation method has been proved as an effective way to obtain highly active electrodes.

In this work, tape casting was applied to prepare a thin scandia stabilized zirconia (SSZ) electrolyte film onto the traditional Ni-yttria stabilized zirconia (YSZ) anode with the thickness of 15 μm. SSZ was used as the electrolyte material due to its high ionic conductivity, chemical stability and mechanical strength at intermediate temperatures. Meanwhile, $Nd_2NiO_{4+\delta}$ (NNO) with high catalytic activity was chosen as the cathode material to reduce the polarization resistance from the cathode. NNO is a mixed electronic and ionic conductor with the K_2NiF_4 type structure belonging to the first order Ruddlesden-Popper family $Ln_2NiO_{4+\delta}$,where Ln is a lanthanide cation such as La, Pr or Nd. It has been reported to exhibit promising electrocatalytic activity for oxygen reduction reaction when used as the cathode of IT-SOFC [14]. The surface exchange coefficient ($K = 10^{-6}$ cm S^{-1}) and oxygen diffusion coefficient ($D^* = 10^{-7}$ cm^2 S^{-1}) are much higher than other perovskite materials, especially at moderate temperatures [15,16]. Furthermore, the Sr-free K_2NiF_4-type cathode material like NNO shows a significantly higher tolerance towards Cr-poisoning [17]. Despite the above merits of NNO as the cathode material of IT-SOFC, the chemical compatibility with traditional electrolyte materials is still a problem. As reported [18], NNO reacts with both CGO and YSZ above a certain temperature (1100 °C and 1000 °C, respectively). In this study, the NNO cathode catalyst was deposited into the pre-sintered SSZ backbones by the impregnation method and calcined at 850 °C. Since the active catalyst was prepared at a relatively low temperature, chemical compatibility problem could be avoided. Also, the resulting nano-micro-structured cathode with high catalytic activity shows promising performance.

2. Experiments

The $Nd_2NiO_{4+\delta}$ (NNO) powder was prepared by a sol–gel combustion method. Stoichiometric amounts of $Nd(NO_3)_3\cdot 6H_2O$ (99%, Sinopharm) and $Ni(NO_3)_2\cdot 6H_2O$ (99%, Sinopharm) were firstly dissolved in deionized water. Citric acid was adopted as the complexing agent and added in a 2:1 molar ratio of citric acid to the total metal ions. The PH value was adjusted to ≈8.5 via the addition of ammonia. After heating and stirring the solution at 90 °C for about 4 h, the green gel was obtained. Then the gel was dried on a hotplate at 220 °C for 6 h to get the self-combusted ash. Finally, in order to investigate the phase formation temperature, the NNO powder was synthesized by calcining the ash at 900–1050 °C in air for 6 h. Commercial YSZ ($(ZrO_2)_{0.92}(Y_2O_3)_{0.08}$, Tosoh/TZ-8Y), CGO ($Ce_{0.9}Gd_{0.1}O_{1.95}$, Ruier, China), SSZ ($Zr_{0.89}Sc_{0.1}Ce_{0.01}O_{2-x}$, Daiichi kigenso kagaku kogyo, Japan) and LSGM ($La_{0.95}Sr_{0.05}Ga_{0.9}Mg_{0.1}O_{0.92}$, Ruier, China) powders were used for the reactivity tests. The mixtures of NNO calcined at 1000 °C for 6 h with the above electrolyte materials were grinded and annealed at temperatures between 1000 and 1200 °C for 5 h, followed by the XRD measurements. The as-synthesized NNO powder was compacted into a cuboid and sintered in air for 6 h at 1000 °C and 1400 °C, respectively. The thermal expansion measurement of the NNO was performed with a dilatometer (NETZSCHDIL402PC) on cuboid specimens from 25 °C to 1000 °C and the electrical conductivity of the NNO was measured in ambient air from 600 to 800 °C using the standard four-probe DC method.

For the symmetrical cathode cells, the tri-layer structure of porous SSZ | dense SSZ | porous SSZ was manufactured by laminating the three tape-cast green tapes. The laminated green tapes were co-sintered at 1400 °C for 4 h in air. Then the NNO catalyst was introduced into the porous SSZ backbones on both sides by impregnating an aqueous solution containing $Nd(NO_3)_3\cdot 6H_2O$, $Ni(NO_3)_2\cdot 6H_2O$ and citric acid in a molar ratio of 2:1:3, followed by calcinating at 850 °C for 2 h in air. The loading of impregnated catalyst was controlled by a micro-liter syringe each time and the impregnation/heat treating cycle was repeated to achieve the ultimate loading needed. A single impregnation/heat treating cycle yielded the loading of ≈5 wt% for the cathode and the ultimate amount of the impregnated catalyst is about 30 wt% as we optimized previously [19].

The single solid oxide fuel cells concerned with this work are planar anode supported cells containing NiO-YSZ anode support layer, NiO-YSZ anode active layer, SSZ electrolyte layer and SSZ cathode backbone layer. The four-layer structure was also prepared by the tape casting and laminating method, followed by a co-sintering process conducted at 1400 °C for 4 h in air. The NNO cathode was impregnated into the SSZ cathode backbone and calcinated at 850 °C for 2 h in air, the same way as for the symmetrical cells.

For electrochemical measurements, silver ink was applied on the electrode surfaces as the current collector. For the single cells, the current–voltage curve and electrochemical impedance spectra were obtained using an IM6 Electrochemical Workstation (ZAHNER, Germany) with one side exposed to air and the other to humidified (3% H_2O) hydrogen, both at a flow rate of 100 mL min^{-1}. The frequency range for impedance measurement was 50 mHz–100 kHz with a 20 mV AC amplitude. Both the active area of the symmetrical cathode cell and the single cell were 0.35 cm^2. The cell structure was examined after testing using scanning electron microscopy (SEM) in a Hitachi S-4800-II microscope.

3. Results and discussion

In order to identify the optimized temperature of the formation of the NNO single phase, NNO powder has been successfully synthesized via the sol–gel combustion method. Fig. 1 shows the XRD patterns of the NNO powders after calcination in air at 900, 950, 1000, 1050 and 1200 °C for 4 h, respectively. The as-prepared oxides exhibited a K_2NiF_4-type structure at all temperature range. From the analyses we can conclude that Nd_2O_3 is the main impurity at 900 and 950 °C. It shows that the lowest phase formation temperature is 1000 °C and the phase is also stable at 1200 °C. The obtained values agree well with those published previously [14,20].

The chemical compatibility with the electrolyte materials has also been discussed. The XRD patterns of the NNO/YSZ, NNO/SSZ, NNO/CGO and NNO/LSGM powder mixtures at different treatment temperatures are shown in Fig. 2. For the NNO/YSZ mixture (Fig. 2(a)), some reaction peaks identified as $Nd_2Zr_2O_7$ and NiO

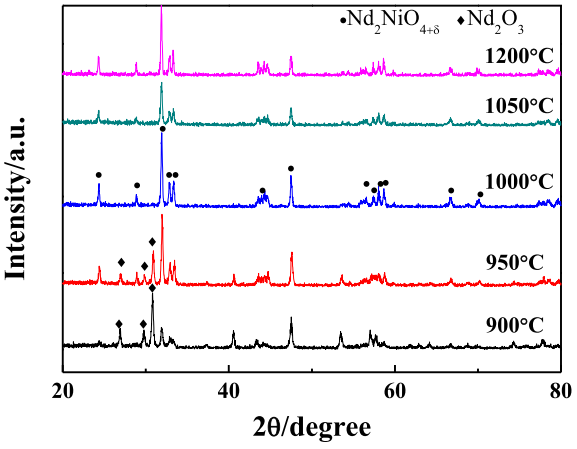

Fig. 1. XRD patterns of the NNO powder sintering at different temperatures.

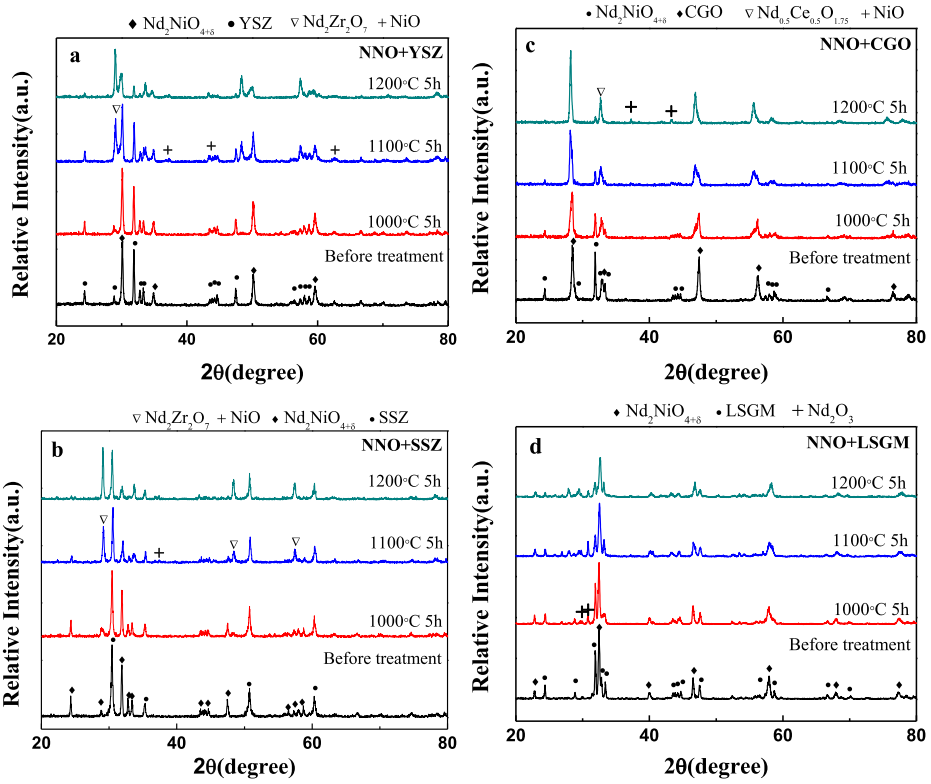

Fig. 2. X-Ray diffraction patterns collected from: (a) NNO/YSZ, (b) NNO/SSZ, (c) NNO/CGO, (d) NNO/LSGM powder mixtures after different heat treatments.

show up after annealing at 1100 °C, the extremely weak peak of $Nd_2Zr_2O_7$ pyrochlore phase is observed at 1000 °C after annealing for 5 h, showing the same result with that obtained from Alejandra Montenegro-Hernandez [18]. In the case of the NNO/SSZ mixture shown in Fig. 2(b), no obvious chemical reaction evidence with electrolyte material or phase decomposition of nickelate was observed by XRD at 1000 °C. However, the peaks of $Nd_2Zr_2O_7$ are clear whereas the intensity of NNO peaks has decreased at 1100 °C after annealing for 5 h. As for the NNO/CGO powder mixture (Fig. 2(c)), no reaction is evident after the 5 h heat treatment conducted at 1100 °C. However, after annealing at 1200 °C for 5 h, two reflections identified as $Nd_{0.5}Ce_{0.5}O_{1.75}$ (▽) and NiO (+) are observed [18,21,22]. Fig. 2(d) exhibits the result of the NNO/LSGM powder mixture. After annealing at 1000 °C for 5 h, the patterns of the mixture show a decrease of the NNO reflections along with the extremely weak peak of Nd_2O_3 (+). These results show that the reactivity at 1000–1100 °C with the electrolyte materials is a drawback. Therefore, the impregnated NNO-SSZ composite cathode was proposed in this work to reduce the sintering temperature and prevent the reaction.

Thermal expansion measurement of the NNO was carried out in the temperature range of 25–1200 °C using a differential dilotameter. The NNO powder was prepared by the sol–gel method. The final annealing was performed at 1000 °C for 6 h to obtain a pure phase. The thermal expansion coefficient (TEC) has been measured in order to evaluate the mechanical compatability with the usual electrolyte materials. Fig. 3 shows that the TEC of the NNO is $13.45 \times 10^{-6}\ K^{-1}$, which is comparable with the results as reported [16,23]. Although it is slightly higher than that of SSZ, it is much

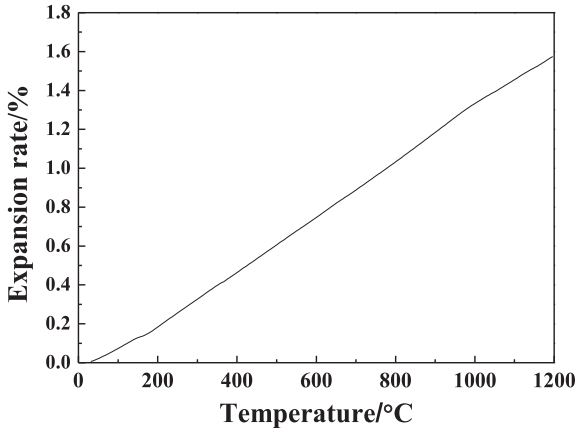

Fig. 3. Line thermal expansion curve for NNO measured at 20–1200 °C.

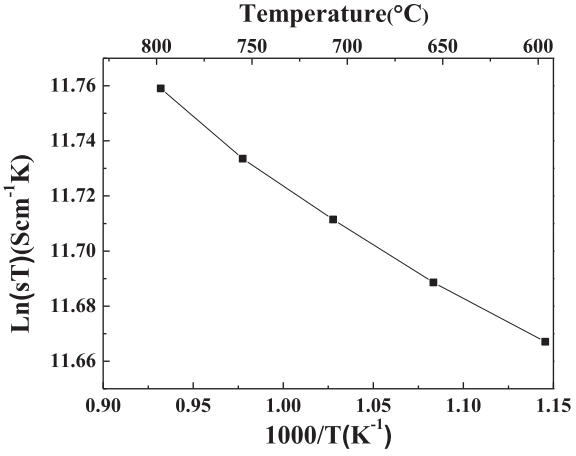

Fig. 4. Electrical conductivity of the NNO measured in air at 600–800 °C.

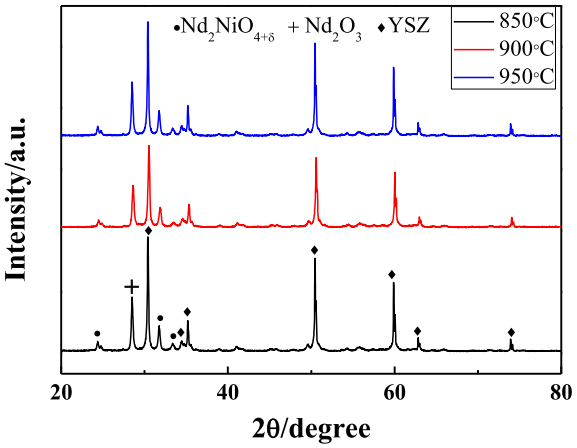

Fig. 5. XRD patterns of the NNO impregnated YSZ composite measured at 850, 900 and 950 °C.

lower than the traditional cathode materials, such as LSCF (24.5×10^{-6} K^{-1}) [24] and so on. Meanwhile, since the NNO catalyst applied here are impregnated onto the inter surface of the SSZ backbone instead of the normal screen printing method, the TEC mismatch may not be a problem [17].

Fig. 4 shows the temperature dependence of the total electrical conductivity of NNO measured in air. The compound exhibits a semi-conducting behavior over the whole temperature rang from 600 to 800 °C. The total conductivity of NNO varies between 133.6 and 119.2 S cm^{-1} at 600–800 °C, which is a little higher than the previous results reported by E. Boehm [16]. Meanwhile, the conductivity increases with temperature decreasing due to a diffusive-type charge transport in the high temperature range. Some researchers have reported that both the decrease of oxygen content and the density of Ni^{3+} carriers have an effect on the conductivity [16,25,26], which further confirmed that NNO is a feasible cathode material applied at intermediate temperature.

Fig. 5 shows the XRD patterns of the NNO impregnated YSZ composite obtained from the symmetrical cells after calcining at 850, 900 and 950 °C for 2 h respectively. We can conclude that the desired NNO phase can be formed at the calcination temperature of 850 °C. However, even improving the calcination temperature to 950 °C, there is still some unreacted Nd_2O_3. Migue A. laguna-Bercero also reported the appearance of Nd_2O_3 after heating at 1000 °C for 2 h, while it does not affect the cathode performance [20].

Fig. 6(a) shows the microstructure of a cross-sectional SEM micrograph of the anode-supported single cell, consisting of a porous NNO impregnated SSZ composite cathode, a dense SSZ electrolyte, a porous Ni-YSZ anode active layer and a porous Ni-YSZ anode substrate. We can note that the thickness of the cell component is about 60, 15, 15 and 600 μm for cathode, electrolyte, anode and anode-support layer, respectively. In both cases, the electrode layers are porous and the adherence with the dense electrolyte is very good. The porous anode active layer (NiO-YSZ) was shown in Fig. 6(b). Fig. 6(c) shows the SEM image of the NNO impregnated SSZ composite cathode at a mass loading of 30 wt%, which exhibits a thin porous and well intra-connected NNO coating on the internal surface of the porous SSZ backbone. A high magnification SEM micrograph of the nano-NNO particles (40–100 nm) was shown in Fig. 6(d). Such a nano-structure has substantially larger surface area than that of the traditional micron-scale cathode and therefore allows for high reduction kinetics [27].

In order to examine the electrochemical behavior of the NNO impregnated SSZ cathode, the typical impedance spectra for such cathode is investigated based on a symmetrical cell was shown in Fig. 7. By introducing the impregnating method, the polarization resistance (Rp) of the symmetrical cell is only 0.04, 0.059, 0.093 and 0.166 Ω cm^2 at 800, 750, 700 and 650 °C respectively, which shows much higher performance compare to other methods. For example, D. Mesguich has reported a NNO symmetrical cell with the polarization resistance of 0.5 Ω cm^2 at 700 °C prepared by the spray pyrolyzed [28]. Spin coating was also applied to fabricate the $Nd_{1.8}Ce_{0.2}Cu_{1-x}Ni_xO_{4+\delta}$ symmetrical cathodes and the minimum

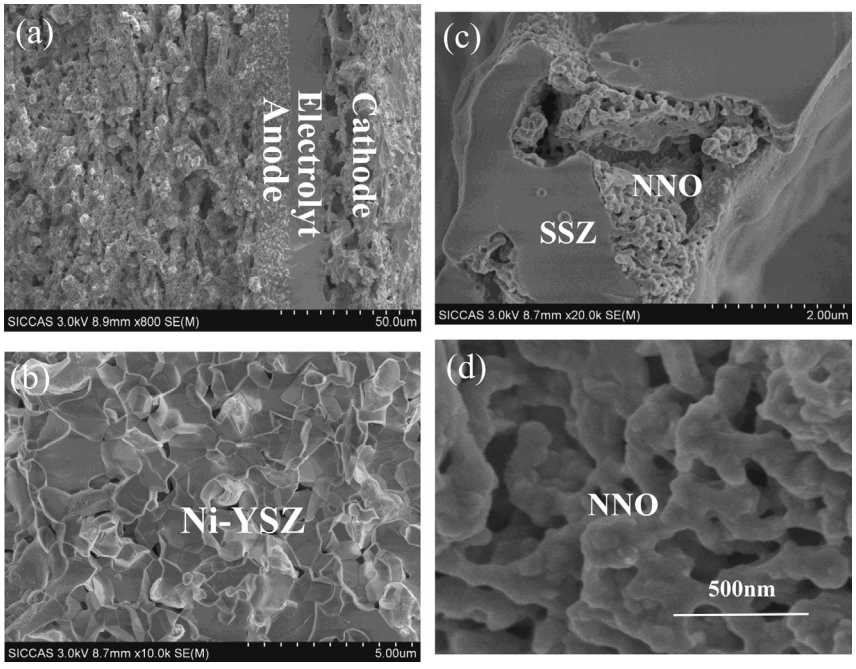

Fig. 6. SEM micrograph of the (a) Single cells after measurement, (b) Ni-YSZ active anode, (c) Impregnated NNO-SSZ cathode and (d) Impregnated NNO particles.

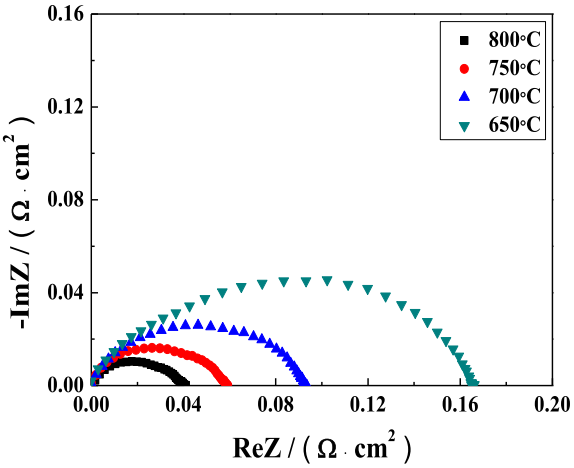

Fig. 7. Electrochemical impedance spectra (EIS) of the symmetrical NNO-SSZ cathode cell measured at 650–800 °C.

area specific resistance (ASR) value of 0.44 Ω cm^2 was obtained at 700 °C [29]. The other $Nd_{1.6}Sr_{0.4}NiO_4$ cathode has showed a performance of 0.93 Ω cm^2 at 700 °C reported by Li-Ping Sun [30]. The much higher performance obtained here may be caused by the impregnated nano-sized NNO particles, which can greatly accelerate the oxygen dissociation and diffusion processes. Most significantly, the cathode polarization performance of the NNO-impregnated SSZ composite cathode reported in this study shows comparable performance with those of LNF (0.054–0.702 Ω cm^2 at 800-650 °C), LSCF, and LSF (0.1 Ω cm^2 at 800 °C) cathodes which were also prepared by the impregnation method [31–33].

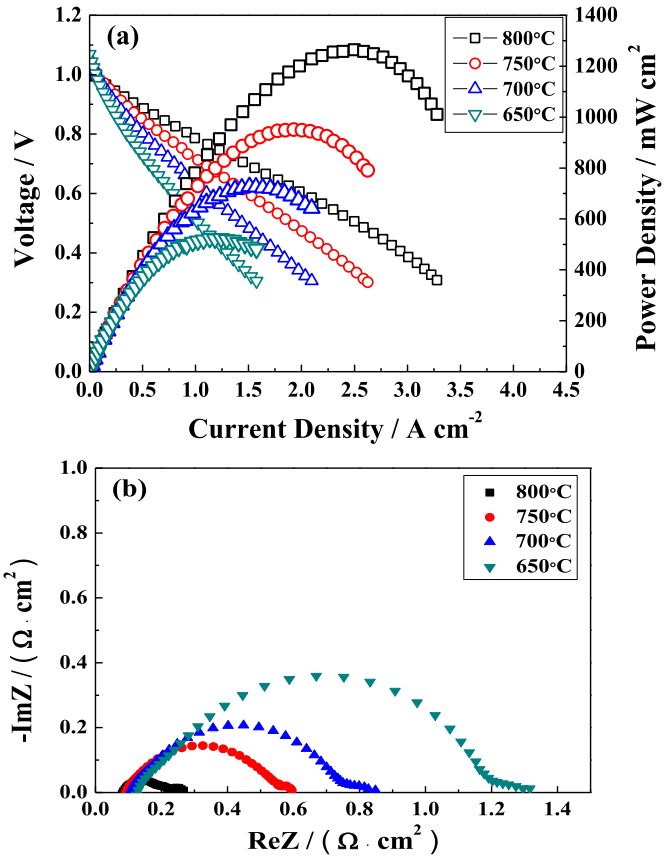

Fig. 8. (a) Voltage and power density versus current density for the present single cell measured at 650–800 °C and (b) Electrochemical impedance spectra measured at open circuits.

The performance of NNO impregnated SSZ cathode is further investigated in a single cell with Ni-YSZ anode and SSZ electrolyte. Electrochemical performance measurements were measured on the single cells with humidified hydrogen fuel and air oxidant at 800 °C-650 °C. Fig. 8(a) shows the typical *i–v* curve for the NNO-SSZ/SSZ/NiO-YSZ/NiO-YSZ cell. The maximum power densities measured are 1.26, 0.95, 0.73 and 0.52 W cm^{-2} at 800, 750, 700 and 650 °C respectively. The performance obtained here is much higher than those reported for the fuel cells with NNO-based cathode and zirconia-based electrolyte. Miguel A. Laguna-Bercero has reported an anode supported micro-tube cell with infiltrated NNO cathode which showed a power density of 0.76 W cm^{-2} at 800 °C [20]. The power density of the single cell with YSZ electrolyte and screen printed $Nd_{1.95}NiO_{4+\delta}$ cathode is only about 90 mW cm^{-2} at 750 °C reported by C. Lalanne [34]. The performance obtained here is also comparable to the intermediate temperature SOFC with impregnated $La_{0.6}Sr_{0.4}Co_{0.2}Fe_{0.8}O_3$ cathode [35,36]. The results indicate that the performance can be improved by impregnating the nano-catalyst and optimizing the electrode microstructure. Fig. 8(b) shows the Nyquist plots of the impedance data obtained at open circuits for the present SOFC. All plots featured large high-frequency arcs and small low-frequency arcs, where the high frequency arc increased much more obviously than the low frequency with decreasing temperature. The overall polarization resistances are 0.19, 0.51, 0.74 and 1.18 Ω cm^2 at 800, 750, 700 and 650 °C respectively as shown in Fig. 8(b), which is lower than the Ni-CGO/YSZ/NNO cell reported by F. Chauveau [37].

4. Conclusions

In the present study, we have shown the good structural stability and reasonable conductivity of the mixed-conducting NNO cathode material. Nano-scale NNO impregnated SSZ composite cathode exhibits high catalytic activity for oxygen reduction, which is desirable to solve the problem of thermal and mechanical mismatching. The area specific polarization resistances of the composite cathode can be as low as 0.04, 0.059, 0.093 and 0.166 Ω cm^2 at 800, 750, 700 and 650 °C respectively. We further demonstrate that an anode supported cell with the NNO-impregnated SSZ composite cathode exhibits an outstanding power density at 800 °C, e.g., 1.26 W cm^{-2}.

Acknowledgment

We gratefully acknowledge the financial support from the Chinese Government High Tech Developing Project (2011AA050702) and the National Natural Science Foundation of China (No. 51172266).

References

[1] S.D. Park, J.M. Vohs, R.J. Gorte, Nature 404 (2000) 265–267.
[2] S.C. Singhal, Solid State Ionics 152 (2002) 405–410.
[3] E.P. Murray, T. Tsai, S.A. Barnett, Nature 400 (1999) 649–651.
[4] Z. Zhan, D.M. Bierschenk, J.S. Cronin, S.A. Barnett, Energy Environ. Sci. 4 (2011) 3951–3954.
[5] T. Hibino, A. Hashimoto, T. Inoue, J. Tokuno, S. Yoshida, M. Sano, Science 288 (2000) 2031–2033.
[6] Y. Chen, Q. Liu, Z. Yang, F. Chen, M. Han, RSC Adv. 2 (2012) 12118–12121.
[7] Y. Takagi, B.-K. Lai, K. Kerman, S. Ramanathan, Energy Environ. Sci. 4 (2011) 3473–3478.
[8] T. Ishihara, J. Yan, H. Matsumoto, ECS Trans. 7 (2007) 435–442.
[9] B. Steele, Solid State Ionics 129 (2000) 95–110.
[10] T. Ishihara, H. Matsuda, Y. Takita, J. Am. Chem. Soc. 116 (1994) 3801–3803.
[11] K. Huang, J.B. Goodenough, J. Alloys Compd. 303–304 (2000) 454–464.

[12] Z.P. Shao, S.M. Haile, Nature 431 (2004) 170–173.
[13] E.D. Wachsman, K.T. Lee, Science 334 (2011) 935–939.
[14] F. Mauvy, Solid State Ionics 158 (2003) 17–28.
[15] E. Boehm, J.M. Bassat, M.C. Steil, P. Dordor, F. Mauvy, J.C. Grenier, Solid State Sci. 5 (2003) 973–981.
[16] E. Boehm, J. Bassat, P. Dordor, F. Mauvy, J. Grenier, P. Stevens, Solid State Ionics 176 (2005) 2717–2725.
[17] M. Yang, E. Bucher, W. Sitte, J. Power Sources 196 (2011) 7313–7317.
[18] A. Montenegro-Hernández, J. Vega-Castillo, L. Mogni, A. Caneiro, Int. J. Hydrogen Energy 36 (2011) 15704–15714.
[19] Y.C. Zhou, X.F. Ye, J.L. Li, Z.L. Zhan, S.R. Wang, J. Electrochem. Soc. 161 (2014). F332–F6.
[20] M.A. Laguna-Bercero, A.R. Hanifi, H. Monzon, J. Cunningham, T.H. Etsell, P. Sarkar, J. Mater. Chem. A 6 (2014) 9764–9770.
[21] I.E.L. Stephens, J.A. Kilner, Solid State Ionics 177 (2006) 669–676.
[22] A. Montenegro-Hernández, L. Mogni, A. Caneiro, Int. J. Hydrogen Energy 37 (2012) 18290–18301.
[23] M. Letilly, A. Le Gal La Salle, M. Caldes, M. Marrony, O. Joubert, Fuel Cells 9 (2009) 622–629.
[24] G. Corbel, S. Mestiri, P. Lacorre, Solid State Sci. 7 (2005) 1216–1224.
[25] J.M. Bassat, P. Odier, J.P. Loup, J. Solid State Chem. 110 (1994) 124–135.
[26] J. Wan, J. Goodenough, J. Zhu, Solid State Ionics 178 (2007) 281–286.
[27] Y. Zhou, X. Xin, J. Li, X. Ye, C. Xia, S. Wang, et al., Int. J. Hydrogen Energy 39 (2014) 2279–2285.
[28] D. Mesguich, J.M. Bassat, C. Aymonier, A. Brüll, L. Dessemond, E. Djurado, Electrochim. Acta 87 (2013) 330–335.
[29] A.P. Khandale, S.S. Bhoga, R.V. Kumar, Solid State Ionics 238 (2013) 1–6.
[30] L.-P. Sun, Q. Li, H. Zhao, L.-H. Huo, J.-C. Grenier, J. Power Sources 183 (2008) 43–48.
[31] B. Huang, X-j Zhu, H-w Nie, Y-r Niu, Y. Li, N. Cheng, J. Power Sources 235 (2013) 20–28.
[32] S.R. Gandavarapu, K. Sabolsky, K. Gerdes, E.M. Sabolsky, Mater. Lett. 95 (2013) 131–134.
[33] Y.Y. Huang, J.M. Vohs, R.J. Gorte, J. Electrochem. Soc. 151 (2004) A646–A651.
[34] C. Lalanne, F. Mauvy, E. Siebert, M.L. Fontaine, J.M. Bassat, F. Ansart, et al., J. Eur. Ceram. Soc. 27 (2007) 4195–4198.
[35] J. Chen, F. Liang, D. Yan, J. Pu, B. Chi, J. San Ping, et al., J. Power Sources 195 (2010) 5201–5205.
[36] M.F. Han, Z. Liu, J. Qian, ECS Trans. 35 (2011) 2295–2303.
[37] F. Chauveau, J. Mougin, J.M. Bassat, F. Mauvy, J.C. Grenier, J. Power Sources 195 (2010) 744–749.